i. Title:

Mutations close to the peptidoglycan-binding region of the stators of the bacterial flagellar motor influence phenamil resistance

ii. Running Title:
Mutants in PG-binding motif of MotB influence phenamil resistance

iii. Authors: The full names of the authors;

Tsubasa Ishida[#1], Rie Ito[#1], Jessica Clark[2], Nicholas J Matzke[3], Yoshiyuki Sowa[*1,4], Matthew AB Baker[*2]
[#] equal contribution
[*] joint corresponding authors

iv. Contact Information:

[1] Department of Frontier Bioscience, Hosei University, Tokyo, Japan.
[2] School of Biotechnology and Biomolecular Science, University of New South Wales, Kensington, NSW, Australia.
[3] School of Biological Sciences, University of Auckland, Auckland, New Zealand.
[4] Research Center for Micro-Nano Technology, Hosei University, Tokyo, Japan.

v. Keywords:

bacterial motility
flagellar motor
ion channels
phenamil
sodium channels

Summary:

The bacterial flagellar motor (BFM) is a molecular complex which powers the rotation of the filament that propels swimming bacteria. Rotational torque is generated by harnessing the flow of ions through ion channels known as stators which couple the energy from the ion gradient across the inner membrane to rotation of the rotor. Here we used error-prone PCR to introduce single point mutations into the sodium-powered *Vibrio alginolyticus / Eschrichia coli* chimeric stator PotB. We then selected for motors that exhibited resistance to the sodium-channel inhibitor phenamil. We found that single mutations that inferred resistance to phenamil occurred at two sites: 1) the transmembrane domain of PotB, corresponding to the TM region of the PomB stator from *V. alginolyticus*, and 2) near the peptidoglycan (PG) binding region that corresponds to the C-terminal region of the MotB stator from *E. coli.* We corroborated our swim plate observations with single cell rotation assays to confirm that individual cells could drive rotation of flagellar motors in the presence of up to 100 µM phenamil. Our results demonstrate that it is not only the pore region of the stator that moderates the effect of motility in the presence of ion-channel blockers. We hypothesise that mutations in the PG region can allow motors to function in the presence of phenamil by allowing multiple semi-functioning stators to persist on the motor and drive flagellar rotation.

Introduction

Motility imparts a large benefit to organisms competing for sparse nutrients. The bacterial flagellum is the oldest known form of motility (Rossmann and Beeby 2018), consisting of a propeller-like filament that rotates under the power of the bacterial flagellar motor (BFM). The BFM is 40 nm in diameter, powered by ion transit across the cell membrane through the stator protein complex, a heterodimer which forms a selective ion channel that transduces chemical energy into mechanical torque (Minamino et al. 2018). While most stators are proton powered (Sowa and Berry 2008), some from marine habitats are sodium powered (Yorimitsu and Homma 2001), others are powered by both sodium ions and protons (Paulick et al. 2015) and recently some have been discovered that are even powered by large divalent cations (Imazawa et al. 2016). In general, flagellar motors have adapted to function in various environments where bacteria live and survive (Terashima et al. 2017; Rossmann and Beeby 2018; Chaban, Coleman, and Beeby 2018). BFM diversity creates an ideal case study to investigate how macromolecular complexes adapt to different environments.

The majority of motors are powered by either protons or sodium ions. In *E. coli* the energy from the proton-gradient is harnessed by the transit of protons through a heterodimeric stator complex composed of $MotA_4MotB_2$ (Minamino et al. 2018). In *Vibrio* species this heterodimer is the sodium ion-powered $PomA_4PomB_2$. The total complex, in both cases, consists of four transmembrane (TM) domains of the A-subunit, a single TM domain of the B-subunit, and a large periplasmic region of the B-subunit which consists of a plug segment and a peptidoglycan-binding (PG-binding) region (Kojima and Blair 2001; Kojima et al. 2009). Recently, the structural rearrangements in PG-binding and stator activation were resolved, indicating that conformational rearrangements of the linker between the PG-binding region and the TM-domain are critical in stator activation (Kojima et al. 2018).

Whilst crystal structures have been solved for the C-terminal domains of MotB in multiple species (Roujeinikova 2008; Kojima et al. 2009; Zhu et al. 2014), the full structure of the TM-domain in any species has yet to be resolved beyond low-resolution cryoEM of the entire stator complex (Yonekura, Maki-Yonekura, and Homma 2011). Much of our understanding of stator function in the TM-domain relies on mutagenesis (Sharp, Zhou, and Blair 1995; Yakushi et al. 2006). Chimeric B-subunits have been engineered that combine the C-terminal peptidoglycan binding motif of the MotB subunit with the transmembrane domain of PomB that forms the ion-channel (in complex with two subunits of PomA) (Asai et al. 2003) (Fig. 1). These chimeric $PomA_4PotB_2$ stators utilise sodium motive force to drive flagellar rotation and can bind to the peptidoglycan (PG) layer thus enabling *E. coli* to swim under sodium-motive force. They have enabled the function of the motor to be investigated at low sodium concentration, and thus low energisation (Sowa et al. 2005; Lo et al. 2013).

Since this chimeric stator complex is driven by sodium ion flow across the inner membrane, it is natural to examine how sodium channel blockers affect this process. Phenamil, a known sodium-channel blocker (Garvin et al. 1985), has been used to probe sodium-interaction sites in sodium driven motors *in situ* in *Vibrio* species (Sugiyama, Cragoe, and Imae 1988; T. Atsumi et al. 1990). Work in *V. alginolyticus* demonstrated that phenamil resistance could be induced by mutations at the cytoplasmic end of the TM-domain of the stator complex (Kojima et al. 1997, 1999). *V. parahaemolyticus* has been widely studied as a model for dual-powered motility; it has lateral flagella that are proton powered but polar flagellar that are sodium

95 powered (Tatsuo Atsumi, McCarter, and Imae 1992). Directed evolution approaches have
96 been applied to *V. parahaemolyticus* to examine which spontaneous mutations might induce
97 resistance to phenamil (Jaques, Kim, and McCarter 1999). Jaques et al. selected for resistance
98 to phenamil by selecting flagellar motors that were motile in the presence of 40 µM phenamil
99 methanesulfonate, yet interestingly only observed a single mutant in the TM-domain that
100 resulted in phenamil resistance.

101 Here we engineered a plasmid construct with enzyme cut sites adjacent to PotB to examine
102 the effects of randomly generated mutations on motility. We screened using phenamil to
103 measure the frequency and location of mutations that imparted phenamil resistance in the
104 sodium powered $PomA_4PotB_2$ chimera. We induced mutations at a controllable rate using
105 error-prone PCR (EP-PCR) and screened large populations of cells using streaking of
106 transformed EP-PCR product onto swim agar in streaks for screening and subsequent
107 sequencing. This allowed a high-throughput screen to determine which mutations have
108 resulted in strains that were functional in the presence of phenamil. By examining the
109 structural and sequence location of these mutations, we have assembled a model that
110 outlines the relationship between PG-binding and stator activity.

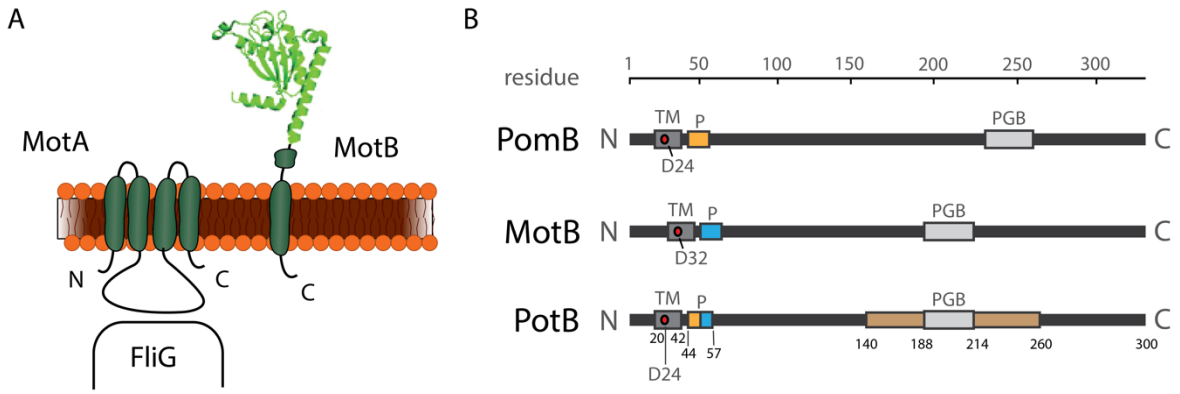

111
112 **Figure 1: Schematic and structure of the stators of the bacterial flagellar motor.** (A) The stator complex in *E.*
113 *coli* consists of a heterodimeric complex composed of $MotA_4MotB_2$. Each stator has two ion channels that are
114 composed of 4 TM domains of MotA and 1 TM domain of MotB. (B) The PotB chimera consists of residues 1-50
115 from V. alginolyticus PomA and residues 59-308 of *E. coli* MotB with TM, plug, PGB and ompA-like regions (brown
116 bar) indicated on the schematic respectively. Structure in A from (Seiji Kojima et al. 2008).
117
118 **Results**
119
120 ***Mutagenesis of PotB.***
121 We generated mutations across the entirety of the PotB protein using error-prone PCR (EP-
122 PCR) as per Methods. We defined the following regions across the PotB protein (numbering
123 via PotB residue number): the TM domain (20-42), the plug (44-57), the middle domain (57-
124 140) the ompA-like domain (140-260) and the peptidoglycan binding domain (188-214). We
125 screened the combinatoric pool of mutagenesis outputs using swim streaking (Fig. S1) and
126 characterised the motility of 27 EP-PCR plasmids that exhibited some motility when selected
127 against phenamil resistance (Fig. S2; Table S1). The distribution of all mutations in all 27
128 plamsids, including silent mutations, is shown in Fig. 2.

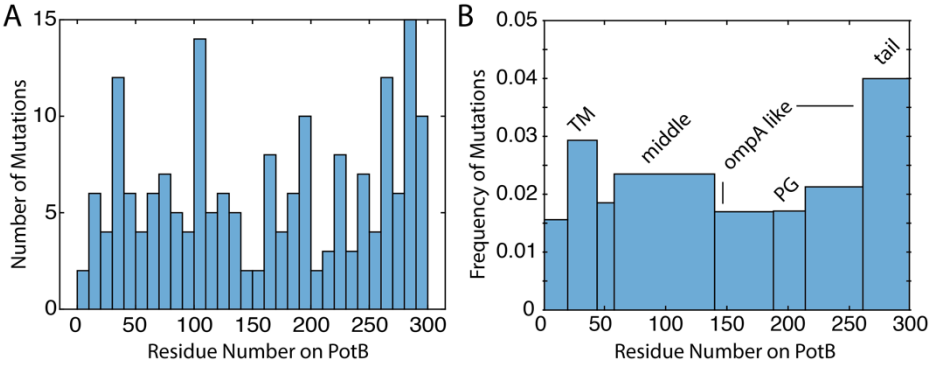

Figure 2: Histogram of mutant frequency. Histograms of mutations from EP-PCR across every strain with at least partial motility in phenamil (from spread plate). (A) Binned evenly across PotB with each bin 10 residues in width showing raw counts of mutations across aggregated results from all 27 EP-PCR plasmids. (B) Frequency of mutations binned according to specific regions of PotB: TM (20-42), plug (44-57), middle (58-139), ompA-like first section (140-187), PG region (188-214), ompA-like second section (215-260) and tail (261-300). Counts are normalised across each region and strain (average mutations per residue per strain).

Together, these histograms indicated that the mutations occurred roughly evenly throughout the protein. When categorised across regions of the protein (Fig. 2B), we observed that proportionately more mutations occurred in screened plasmids in the TM and the tail region of PotB.

Point mutations in TM domain can impart phenamil resistance.

Out of the 27 strains (Table S1), six exhibited a strong motility phenotype when motility was characterised in the presence of 20 µM phenamil. Of particular interest, we focused on plasmid PotB-ep18 (Fig. S1-S2, Table S1) which contained only 3 mutations: F22Y, L28Q, K100Q and demonstrated increased motility in the presence of phenamil. To address the relative contributions of each mutation to the observed phenotype we synthesised single point mutants of each of the three mutations (Fig. S3). Both F22Y and L28Q alone imparted phenamil resistance to PotB (Fig. 3), or together (pSHU149, F22Y/L28Q). Mutation K100Q appeared to offer no phenamil resistance and as such was classified a redundant mutation. These results indicate that single point mutations, particularly in the pore region of the TM domain of PotB, can impart phenamil resistance.

Point mutations near PG-binding domain can impart phenamil resistance.

Plasmid PotB-ep9 (Fig. S1-S2; Table S1) displayed a phenamil-resistant phenotype and also had only three mutations: Y163F, M164V and L255M. This was targeted for further investigation as these mutations were all far from the TM domain. We again characterised the contributions of each mutation to motility and observed that Y163F and M164V each separately induce phenamil resistance and that L255M was a redundant mutation (Fig. S3). When both mutations were combined in a single plasmid (pSHU146), phenamil-resistance was increased (Fig. 3).

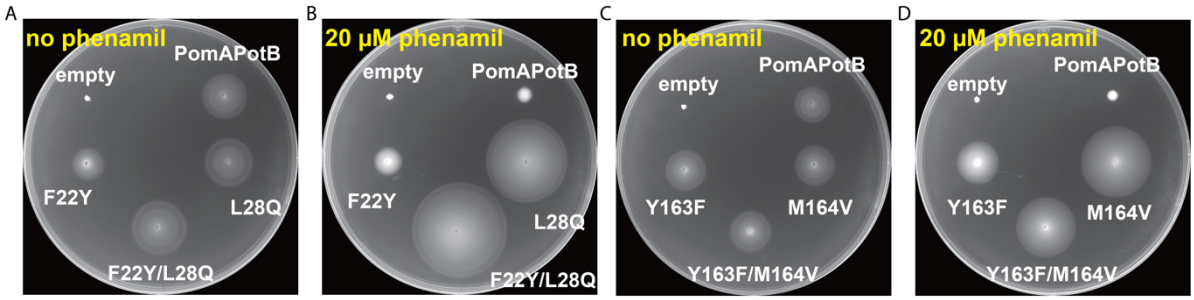

Figure 3: Mutants in TM-domain and PG-binding region induce phenamil resistance. Motility of either TM-domain mutants (A/B) or PG-binding mutants (C/D) was tested via 0.25% agar swim plating using the empty vector (pBAD33) and PomAPotB wild-type as a negative and positive control respectively. A/C) In the absence of phenamil, swimming of mutants is comparable to the positive control. B/D) In the presence of 20 µM phenamil, the mutants are motile whilst PomAPotB wild-type is severely limited. A/C incubated at 30˚C for 10 hours, B/D incubated at 30˚C for 18 hours.

PG-binding double mutants rotate at lower sodium concentration than wild-type PotB

To establish whether these mutants were generating torque from sodium motive force, or had undergone a change in ion-specificity, we tested swimming in minimal sodium-free media (Fig. S4). None of the mutants were motile in sodium-free media, yet all plasmids restored swimming in the presence of sodium and in the presence and absence of phenamil (Fig S4). We then tested individual cells for rotation whilst lowering the concentration of sodium to determine whether the dependence on sodium-motive force (SMF) had changed in these mutants (Fig. 4). This allowed us to confirm that our observed swim plate phenotype was caused changes in flagellar rotation, and account for any compensatory changes in growth or chemotaxis that might confound swim plate measurements. We examined the capacity of pSHU1234 and our mutant plasmids to restore swimming in 'sticky-filament' strains. These sticky-filament mutants lack the surface of the protein FliC and thus undergo hydrophobic interactions with glass that enable filaments to stick to glass and allow the rotation of the body to be assessed in parallel (Kuwajima 1988). In comparison with PomAPotB wild-type, the mutants in the PG-region (pSHU146: Y163F/M164V) were highly motile at low sodium, with cells rotating > 6 Hz in the presence of only 0.3 mM Na^+. This is in contrast to PomAPotB wild-type restoring motility to < 2 Hz at the equivalent sodium motive force. In an opposite trend, mutations in the TM region (pSHU149: F22Y/L28Q) did not demonstrate swimming below 1 mM Na^+ and had a lower maximum speed and slower response to increased [Na^+].

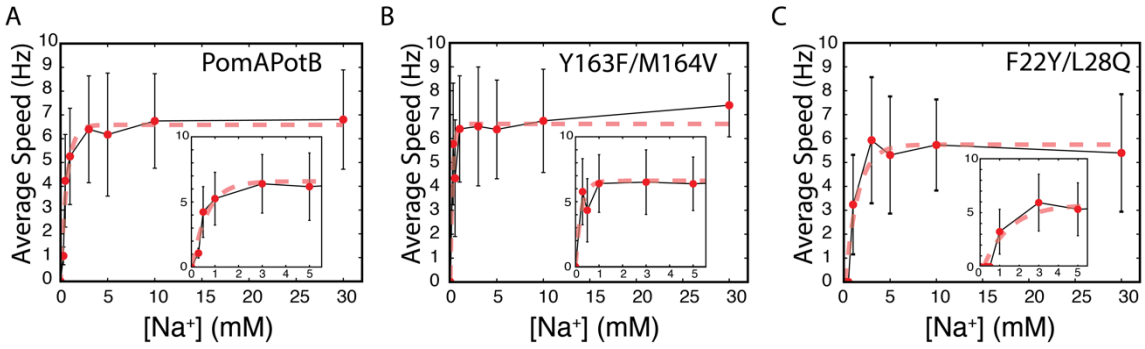

Figure 4: Y163F/M164V is motile at less than 0.3 mM [NaCl]. (A) The PomAPotB wild-type exhibits single cell rotation from 0.3 mM Na^+, increasing exponentially to a plateau above 6 Hz at full energisation. (B) PotB Y163F/M164V displays rotation at 0.3 mM Na^+, with plateau above 6 Hz at full energisation. (C) potB F22Y/L28Q displays no rotation below 1 mM Na^+, with a slower increase to a lower maximum speed plateau above 5 Hz and under 6 Hz. Inset in ABC shows zoom around 0-5 mM [Na^+].

195 ***TM-domain double mutants are not affected by increasing concentrations of phenamil.***
196
197 The response of single-cell speed with varying phenamil concentration was measured to
198 examine the energy profile and structural basis of phenamil resistance in our two phenamil-
199 resistant plasmids. In wild-type PomAPotB tethered cell rotation speed was reduced
200 significantly when as little as 1 µM of phenamil was introduced, and cell speed plateaued at
201 5 µM of phenamil. The PG-binding double mutant (Y163F/M164V) demonstrated the same
202 plateau effect in response to increasing phenamil but the concentration dependence of the
203 decrease in rotational speed was much lower, that is, the decay constants for a
204 monoexponential fit were 0.8 mM^{-1} and 0.2 mM^{-1} for PomAPotB wild-type and Y163F/M164V
205 respectively. Similarly, the I_{50}, the concentrations of phenamil at which the speed was half
206 the maximum, was 0.9 µM and 3.1 µM for wild-type and Y163F/M164V respectively. In
207 contrast, the speed of rotation for the double TM-domain mutant (F22Y/L28Q) exhibited no
208 dependence on phenamil concentration up to 50 µM, and only a 46% reduction on maximum
209 speed at 100 µM phenamil. This implies that the mechanism of resistance in the TM-domain
210 mutants destroyed much of the efficacy of phenamil altogether, whereas the PG-binding
211 region mutants acted to stabilise rotation in the presence of phenamil, but this stabilisation
212 could be overcome as phenamil concentration was increased.
213

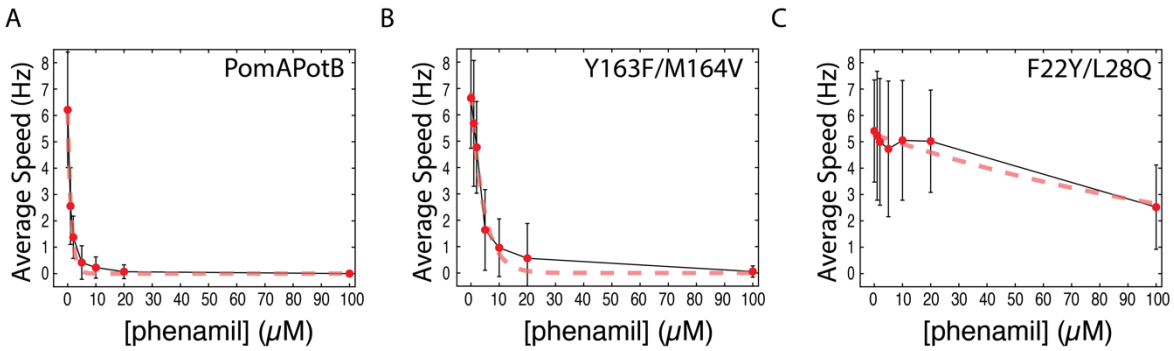

214 **Figure 5: TM mutants impart phenamil resistance up to 100 µM**. Dose response of averaged measurements of
215 single-cell rotation speed with varying concentration of phenamil for: (A) PomAPotB wild-type, (B) double TM-
216 domain mutant (PomAPotB F22Y/L28Q) and (C) double PG-binding mutant (PomAPotB Y163F/M164V). Tethered
217 cell data is fit with monoexponential decay curve to generate time constants for decay (PomAPotB wild-type:
218 0.8 mM^{-1}; PomAPotB Y163F/M164V: 0.2 mM^{-1}; PomAPotB F22Y/L28Q: 0.007 mM^{-1}).
219

F22Y is common and clusters in phylogenies along MotB/PomB lines; L28Q is very rare.

A large low-level phylogeny of 948 MotB homologues was assembled which clearly divided into clades (Fig. 6A). Examination of a curated subset of 32 commonly studied species (Fig. 6B) was examined to look at patterns at the sites of the mutations studied in this work. Parsimony trees were reconstructed at each node of the smaller phylogeny and the sequence identity at each node estimated to map trends in mutation across the phylogeny. At the F22Y site, residues clearly clustered according to MotB/PomB identity (Fig. 6B, left), which is putatively linked to proton/sodium motility. However, at the L28Q site (Fig 6B, right), the 32 curated species did not divide along MotB/PomB lines, in fact these curated species were in most cases leucine and in close relatives of *E. coli* were alanine. In fact, over the entire 948 species in the larger phylogeny, only one species had a glutamine at that site: *Myxococcus fulvus.*

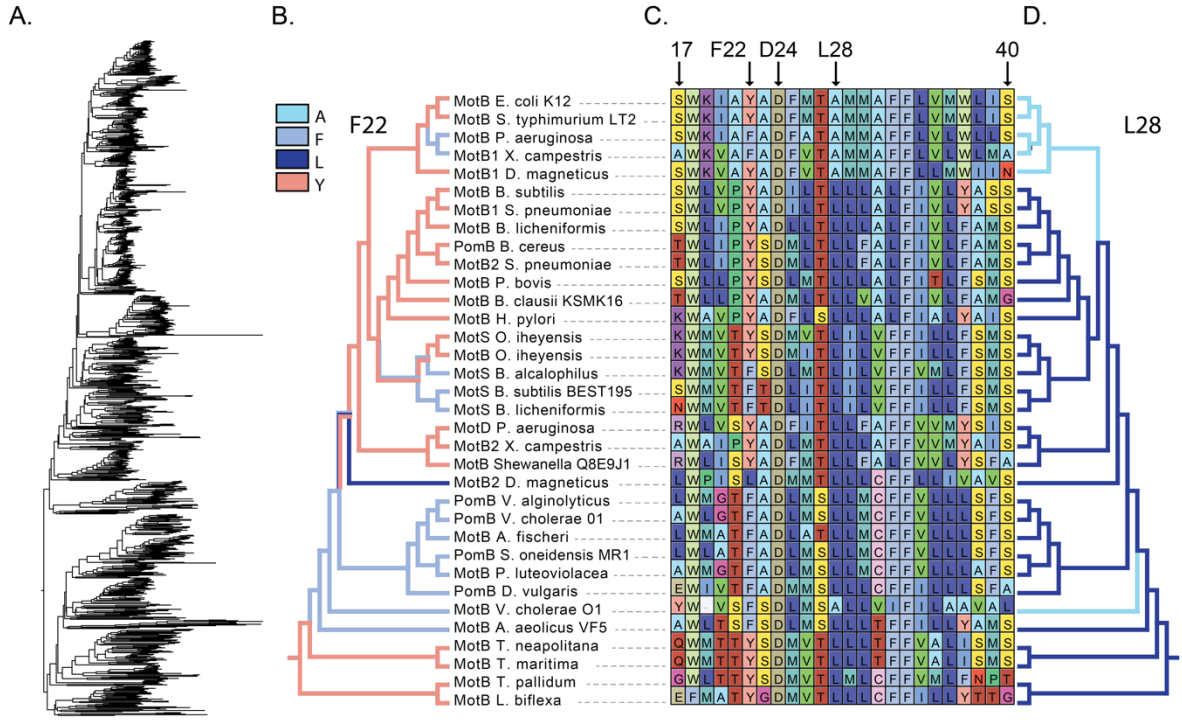

Figure 6: Parsimony Reconstruction for Y22 and L28. (A) Overall phylogeny of 948 MotB homologs showing clear cladding. (B) Parsimony reconstruction for site Y22 (PotB numbering) shown in colour over subset phylogeny of 34 representative species as labelled. (C) Sequence alignment across transmembrane domain of MotB/PomB showing conserved D24, and Y22/L28 mutations tested in this work. (D) Parsimony reconstruction for site L28A (PotB numbering) shown in colour over subset phylogeny.

Y163F/M164V are both rare and do not cluster along MotB/PomB lines.

Similarly, we aligned the sequences in the section 156-214, including the PG-binding site, and performed parsimony reconstructions at each node of our curated phylogeny (Fig. 7). In both Y163F and M164V the mutations did not cluster according to MotB/PomB lines. A phenylalanine at site 163 was very rare across the full phylogeny, occurring only in *Yersinia pestis biovar Orientalis.* The valine at site 163 was observed in 13 species, mostly among members of the *Spirochaetes* and *Oceanospirilla* families (Supplementary Note).

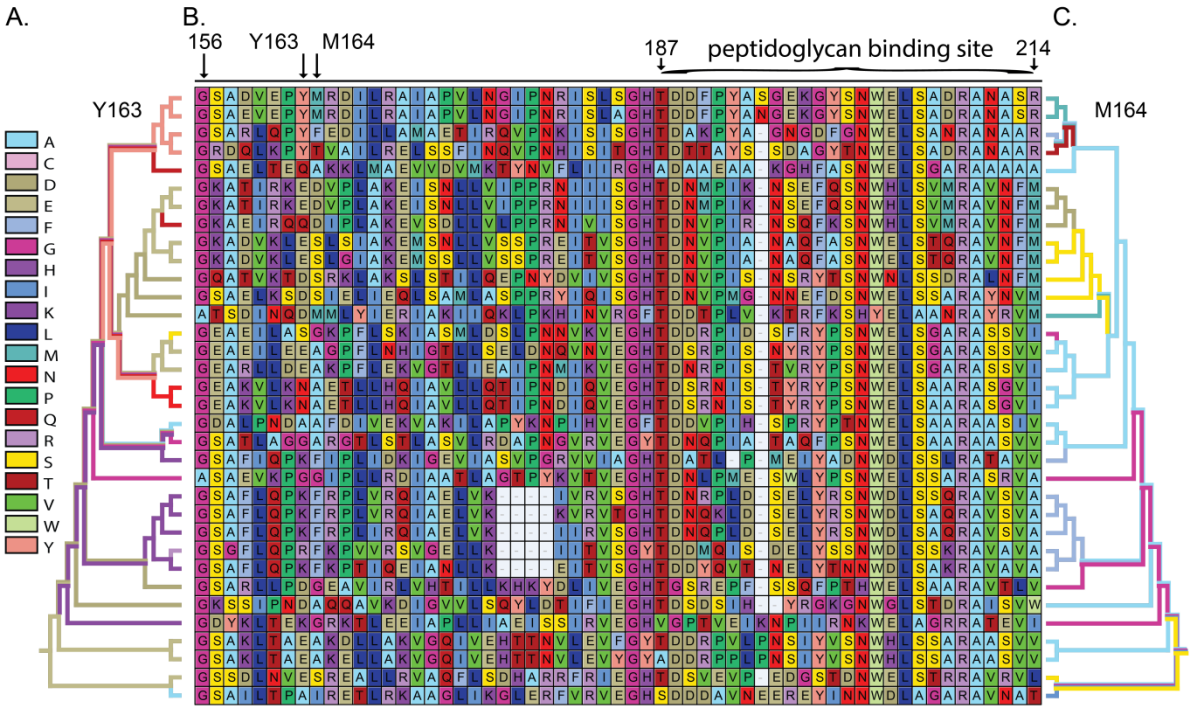

Figure 7: Parsimony Reconstruction for Y163 and M164. (A) Parsimony reconstruction for site Y163 (PotB numbering) shown in colour over subset phylogeny of 34 representative species from Fig. 5. (B) Sequence alignment over peptidoglycan binding site of MotB/PomB showing Y163/M164 mutations tested in this work. (C) Parsimony reconstruction for site M164 (PotB numbering) shown in colour over subset phylogeny.

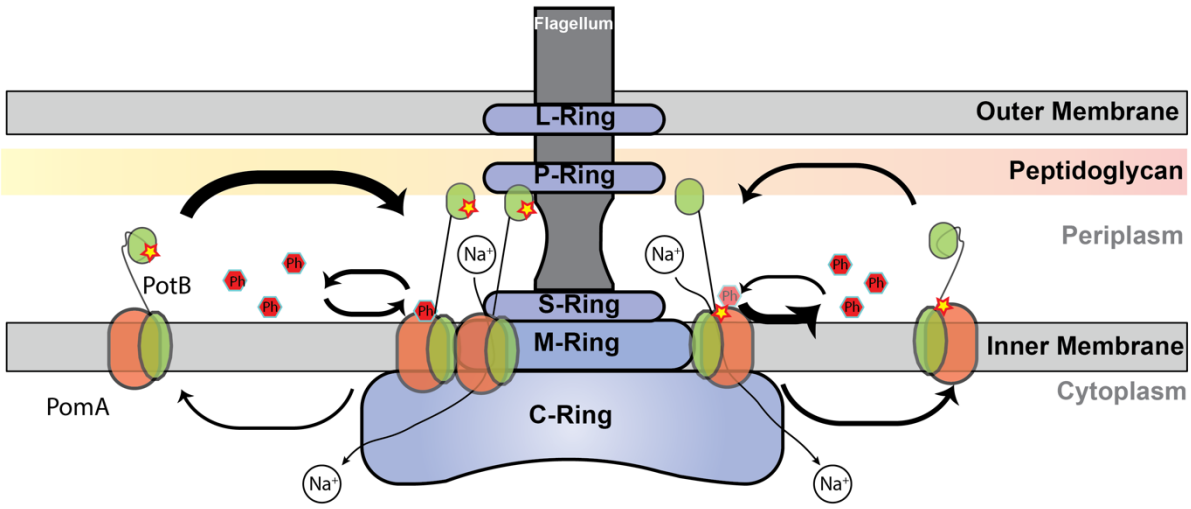

Figure 8: Model of activity. Schematic showing effects of mutations with respect to phenamil and sodium flow through stator complex. The pool of stator complexes ($PomA_4PotB_2$) diffuse in the inner membrane, and when they bind to the motor the PG-binding region pulls with tension on the transmembrane domains of PomA and PotB (Kojima et al. 2018). (left) Mutations in the 163/164 site affect PG-binding and the duration for which a stator is bound to the motor (dwell time). This results in a slower off rate with respect to wild-type stators and a larger steady-state population of stators bound to the motor. In the presence of phenamil each stator has reduced functionality but in sum, with many stators, the motor is functional. (right) Mutations at the TM-domain near the putative phenamil binding site affect the binding and release of phenamil, thus phenamil is bound more weakly, and turns over more rapidly, allowing sodium ions to pass through the channel to generate motor rotation.

Discussion

We have examined the effect of mutations in both the transmembrane domain and the peptidoglycan binding region of PotB. We observed that single point mutations in the TM region at L28 and F22 were sufficient to induce phenamil resistance. The mutation at F22Y is highly clustered around Pom/Mot stator subunits in varying species and presumably linked to sodium/proton specificity, which may show that residue F22 not only plays a role in sodium binding but also phenamil-binding and sodium blocking. Together with a mutation we observed as an EP-PCR product at L28Q, these two mutations enabled phenamil resistance across a large range of phenamil concentrations, with stators remaining functional at concentrations of phenamil as high as 100 µM phenamil. This high tolerance to phenamil implies that they have affected or removed the binding site of phenamil inside the pore region of the stator complex.

Similarly, in the PG-binding region we observed that two clustered single mutations were also sufficient to impart phenamil resistance. The PG-binding region is used to bind the stators in place so that they act on the motor. With these two mutations at Y163/M164 we observed a decaying concentration dependence of rotation to phenamil. These sites are far from the pore, which is expected to be the phenamil binding site, thus we propose that the mechanism of resistance was not related to altering the efficacy of binding of phenamil. We propose that resistance was induced via changes to the binding strength of PotB to the PG layer in *E. coli*. This in turn would be sufficient to alter the dwell time of the stator on the rotor, that is, would result in more stators being bound more often (Fig. 8). In turn, if each stator is fractionally functional, or occasionally able to pass a sodium ion in the presence of phenamil, then in total,

with more stators on the rotor, these sodium-powered flagellar motors are able to function in the presence of phenamil. This model needs to be further tested using single cell studies and combined single molecule fluorescence to quantify exactly and changes in the dwell time of mutant stators on the motor, the on and off rates of the stators binding to the motor, and how these properties change as a function of external sodium concentration.

Phenamil resistance has been studied in other species, most notably in *Vibrio parahaemolyticus*. This system is of interest as it has two motors, one sodium powered and one proton powered and phenamil has been studied previously as a drug target for this pathogen (Tatsuo Atsumi, McCartert, and Imae 1992; Jaques, Kim, and McCarter 1999). Jaques et al. used natural selection over 12-18 days to screen for phenamil resistance (Jaques, Kim, and McCarter 1999). They observed a single mutation in the TM-domain, but did not observe the mutations that we saw in this paper. Their experiment, occuring through natural mutagenesis and evolution in a laboratory setting will respond to pleiotropy and epistasis and also inherent directionality in the process of stator adaptation. This means that the order of specific mutations can restrict the possible outcomes. Naturally, our mutation at L28Q was indeed very rare across our set of 948 MotB homologues, occurring only once in *Myxococcus fulvus* ~0.1% of the species we examined. EP-PCR however, is agnostic to the order of mutations and will insert mutations evenly across the protein of interest. This highlights the power of EP-PCR to explore novel mutations and to compare historical evolutionary occurrences with those that can be discovered via directed and laboratory-assisted experimental evolution.

Our experimental system allows us to examine phenotypes to determine which amino acids have a functional cause in changing a phenotype. This allows us to address a common puzzle in phylogenetics: because both mutations and traits are inherited on the phylogeny, they are non-independent, and can thus exhibit “accidental” correlation without a functional relationship (Uyeda, Zenil-Ferguson, and Pennell 2018). In the case of MotB, every clade has some amino acids unique to it, but this will be true whether or not those residues have a functional role in the clade’s motility phenotype. For example, we can characterise phenamil resistance and adaptation in ion-source to measure whether changes on the phylogeny are associated with a particular ion source, or a particular habitat, across a number of independent transitions. This allows us to quantify which amino acids, potentially in which order, have been part of historic adaptation events such as a transition from sodium to proton-based motility. In turn, we can use these approaches to tease out the causality of events that constrain natural adaptation.

Experimental Procedures

Bacterial strains and plasmids

Bacterial strains and plasmids used in this study are listed in SI. For swim plating, plasmids were transformed into RP6665 (Δ*motAmotB*) (Block, Blair, and Berg 1989) to restore motility. For tethered cell assays, plasmids were transformed into JHC36 (Δ*cheY fliC-sticky* Δ*pilA* Δ*motAmotB*) (Inoue et al. 2008).

Error-prone PCR

Plasmid pSHU1234 was constructed in a pBAD33 backbone with unique cut-sites for NdeI and PstI directly upstream and downstream of PotB. Error-prone PCR was executed on pSHU1234 using primer 1176 and primer 0104 (Table S2), taq polymerase, unbalanced dNTPs and Mn^{2+}, as per (Wilson and Keefe 2000). The post-PCR product and pSHU1234 was then digested and ligated with NdeI and PstI and transformed into RP6665(Δ*motAB*).

Mutant isolation

Tranformant was streaked in lines on low agarose motility plate (Fig. S1) consisting of 0.25% TB soft agar, 25 µg/mL chloramphenicol, 1 mM arabinose and 20 µM phenamil. These plates were incubated at 30˚C for 20 hours. Flares were selected from these plates and single colonies were generated. These colonies were harvested, the plasmid was purified, transformed again into RP6665 and motility was tested as below. Specific mutants derived from EP-PCR outcomes were engineered using a standard site-directed mutagenesis protocol with forward and reverse primers (Supplementary Materials), template, and high-fidelity DNA polymerase (Pfu Ultra).

Motility assays

Motility testing was carried out using motility plate assays. Phenamil to a final concentration of either 0, 20 or 100 µM was added to the plates. Swim plates were inoculated from single colonies by toothpick. Plates were incubated for 10 or 18 hours respectively, as noted. Minimal media for minimal motility assays (Fig. S4) consisted of 10 mM KPO_4, 0.1% glycerol, 0.1 mM Thr, 0.1 mM Leu, 0.1 mM His, 0.1 mM Met, 0.1 mM Ser, 1 mM $MgSO_4$, 1 mM $(NH_2)_2SO_4$, 1 µg/mL Thiamine, 0.5% NaCl or KCl respectively (85 mM [NaCl]; [67 mM KCl]), 1 mM arabinose, 25 µg/mL chloramphenicol and the indicated concentration of phenamil (0, 20, 100 µM).

Sequence analysis

Sequencing was executed commercially by FASMAC (Japan) using forward and reverse primers and template (Table S2). Three primers were used to read the entire PomAPotB region.

Single cell speed assays

Cells were adhered spontaneously to glass coverslips via a sticky-filament and then imaged onto a CMOS camera at 60 frames per second thorough 40x objective. Rotation of tethered sticky-filament cells was analysed using custom software based upon LabView (National Instruments).

372 *Phylogenetics and sequence diversity of MotB homologs*
373 To survey the known flagellar diversity for amino acid substitutions similar to the upmotile
374 mutations discovered by experiment, we estimated a very large phylogeny of MotB and
375 related proteins. As our goal was exploratory, we chose faster heuristic methods feasible for
376 a large dataset, rather than Maximum Likelihood or Bayesian methods that would be
377 impracticably slow. 948 MotB homologs were assembled by searching UniProt90 against key
378 study taxa. They were aligned using Clustal Omega (Larkin et al. 2007) on its most thorough
379 settings (5 iterations of re-alignment). The phylogeny was then estimated with Quicktree, a
380 neighbour-joining method suitable for large datasets (Howe, Bateman, and Durbin 2002). The
381 phylogeny was midpoint-rooted in FigTree (Rambaut 2018). As these are fast heuristic
382 methods based on a single protein, deeper branches and rooting should be considered
383 uncertain, and we make no claim about e.g. inter-phylum relationships, a very difficult
384 phylogenetic problem (Pallen and Matzke 2006; Abby and Rocha 2012; Shih and Matzke 2013;
385 Koonin 2016). However, the tree was adequate for the purpose of showing relationships
386 between close relatives, and for surveying MotB sequence conservation and diversity.
387
388 To further explore conservation and diversity at key positions of the alignment, ancestral
389 amino acids were reconstructed on the phylogeny using parsimony in Mesquite (Maddison
390 and Maddison 2015). The 948-protein tree was subset to key study taxa for Fig. 6 and Fig. 7.
391
392
393 **References**
394
395 Abby, Sophie S., and Eduardo P. C. Rocha. 2012. "The Non-Flagellar Type III Secretion
396 System Evolved from the Bacterial Flagellum and Diversified into Host-Cell Adapted
397 Systems." *PLOS Genetics* 8 (9): e1002983.
398 Asai, Yukako, Toshiharu Yakushi, Ikuro Kawagishi, and Michio Homma. 2003. "Ion-
399 Coupling Determinants of Na+-Driven and H+-Driven Flagellar Motors." *Journal of*
400 *Molecular Biology* 327 (2): 453–63.
401 Atsumi, T., S. Sugiyama, E. J. Cragoe, and Y. Imae. 1990. "Specific Inhibition of the Na(+)-
402 Driven Flagellar Motors of Alkalophilic Bacillus Strains by the Amiloride Analog
403 Phenamil." *Journal of Bacteriology* 172 (3): 1634–39.
404 Atsumi, Tatsuo, Linda McCarter, and Yasuo Imae. 1992. "Polar and Lateral Flagellar Motors
405 of Marine Vibrio Are Driven by Different Ion-Motive Forces." *Nature* 355 (6356):
406 182–84.
407 Block, Steven M., David F. Blair, and Howard C. Berg. 1989. "Compliance of Bacterial
408 Flagella Measured with Optical Tweezers." *Nature* 338 (6215): 514–18.
409 Chaban, Bonnie, Izaak Coleman, and Morgan Beeby. 2018. "Evolution of Higher Torque in
410 Campylobacter-Type Bacterial Flagellar Motors." *Scientific Reports* 8 (January): 97.
411 Garvin, J. L., S. A. Simon, E. J. Jr Cragoe, and L. J. Mandel. 1985. "Phenamil: An
412 Irreversible Inhibitor of Sodium Channels in the Toad Urinary Bladder." *J Membr*
413 *Biol* 87 (1): 45–54.
414 Howe, Kevin, Alex Bateman, and Richard Durbin. 2002. "QuickTree: Building Huge
415 Neighbour-Joining Trees of Protein Sequences." *Bioinformatics* 18 (11): 1546–47.
416 Imazawa, Riku, Yuka Takahashi, Wataru Aoki, Motohiko Sano, and Masahiro Ito. 2016. "A
417 Novel Type Bacterial Flagellar Motor That Can Use Divalent Cations as a Coupling
418 Ion." *Scientific Reports* 6 (January): 19773.
419 Inoue, Yuichi, Chien-Jung Lo, Hajime Fukuoka, Hiroto Takahashi, Yoshiyuki Sowa, Teuta
420 Pilizota, George H. Wadhams, Michio Homma, Richard M. Berry, and Akihiko

Ishijima. 2008. “Torque-Speed Relationships of Na+-Driven Chimeric Flagellar Motors in Escherichia Coli.” *Journal of Molecular Biology* 376 (5): 1251–59.

Jaques, S., Y. K. Kim, and L. L. McCarter. 1999. “Mutations Conferring Resistance to Phenamil and Amiloride, Inhibitors of Sodium-Driven Motility of Vibrio Parahaemolyticus.” *Proceedings of the National Academy of Sciences of the United States of America* 96 (10): 5740–45.

Kojima, S., Y. Asai, T. Atsumi, I. Kawagishi, and M. Homma. 1999. “Na+-Driven Flagellar Motor Resistant to Phenamil, an Amiloride Analog, Caused by Mutations in Putative Channel Components.” *Journal of Molecular Biology* 285 (4): 1537–47.

Kojima, S., T. Atsumi, K. Muramoto, S. Kudo, I. Kawagishi, and M. Homma. 1997. “Vibrio Alginolyticus Mutants Resistant to Phenamil, a Specific Inhibitor of the Sodium-Driven Flagellar Motor.” *Journal of Molecular Biology* 265 (3): 310–18.

Kojima, Seiji, and David F. Blair. 2001. “Conformational Change in the Stator of the Bacterial Flagellar Motor.” *Biochemistry* 40 (43): 13041–50.

Kojima, Seiji, Yukio Furukawa, Hideyuki Matsunami, Tohru Minamino, and Keiichi Namba. 2008. “Characterization of the Periplasmic Domain of MotB and Implications for Its Role in the Stator Assembly of the Bacterial Flagellar Motor.” *Journal of Bacteriology* 190 (9): 3314–22.

Kojima, Seiji, Katsumi Imada, Mayuko Sakuma, Yuki Sudo, Chojiro Kojima, Tohru Minamino, Michio Homma, and Keiichi Namba. 2009. “Stator Assembly and Activation Mechanism of the Flagellar Motor by the Periplasmic Region of MotB.” *Molecular Microbiology* 73 (4): 710–18.

Kojima, Seiji, Masato Takao, Gaby Almira, Ikumi Kawahara, Mayuko Sakuma, Michio Homma, Chojiro Kojima, and Katsumi Imada. 2018. “The Helix Rearrangement in the Periplasmic Domain of the Flagellar Stator B Subunit Activates Peptidoglycan Binding and Ion Influx.” *Structure,* 26 (4): 590-598.e5.

Koonin, Eugene V. 2016. “Horizontal Gene Transfer: Essentiality and Evolvability in Prokaryotes, and Roles in Evolutionary Transitions.” *F1000Research* 5 (July): 1805.

Kuwajima, G. 1988. “Construction of a Minimum-Size Functional Flagellin of Escherichia Coli.” *Journal of Bacteriology* 170 (7): 3305–9.

Larkin, M. A., G. Blackshields, N. P. Brown, R. Chenna, P. A. McGettigan, H. McWilliam, F. Valentin, et al. 2007. “Clustal W and Clustal X Version 2.0.” *Bioinformatics* 23 (21): 2947–48.

Lo, Chien-Jung, Yoshiyuki Sowa, Teuta Pilizota, and Richard M. Berry. 2013. “Mechanism and Kinetics of a Sodium-Driven Bacterial Flagellar Motor.” *Proceedings of the National Academy of Sciences of the United States of America* 110 (28): E2544–51.

Maddison, WP, and DP Maddison. 2015. *Mesquite: A Modular System for Evolutionary Analysis. Version 3.04*. https://www.mesquiteproject.org/.

Minamino, Tohru, Naoya Terahara, Seiji Kojima, and Keiichi Namba. 2018. “Autonomous Control Mechanism of Stator Assembly in the Bacterial Flagellar Motor in Response to Changes in the Environment.” *Molecular Microbiology* 109 (6): 723–34. https://doi.org/10.1111/mmi.14092.

Pallen, Mark J., and Nicholas J. Matzke. 2006. “From The Origin of Species to the Origin of Bacterial Flagella.” *Nature Reviews. Microbiology* 4 (10): 784–90. https://doi.org/10.1038/nrmicro1493.

Paulick, Anja, Nicolas J. Delalez, Susanne Brenzinger, Bradley C. Steel, Richard M. Berry, Judith P. Armitage, and Kai M. Thormann. 2015. “Dual Stator Dynamics in the Shewanella Oneidensis MR-1 Flagellar Motor.” *Molecular Microbiology* 96 (5): 993–1001.

Rambaut, Andrew. (2015) 2018. *FigTree v1.4.4, a Graphical Viewer of Phylogenetic Trees. 2014*. Java. https://github.com/rambaut/figtree.

Rossmann, F. M., and M. Beeby. 2018. "Insights into the Evolution of Bacterial Flagellar Motors from High-Throughput in Situ Electron Cryotomography and Subtomogram Averaging." *Acta Crystallographica Section D: Structural Biology* 74 (6): 585–94.

Roujeinikova, Anna. 2008. "Crystal Structure of the Cell Wall Anchor Domain of MotB, a Stator Component of the Bacterial Flagellar Motor: Implications for Peptidoglycan Recognition." *Proceedings of the National Academy of Sciences* 105 (30): 10348–53.

Sharp, Leslie L., Jiadong Zhou, and David F. Blair. 1995. "Tryptophan-Scanning Mutagenesis of MotB, an Integral Membrane Protein Essential for Flagellar Rotation in Escherichia Coli." *Biochemistry* 34 (28): 9166–71.

Shih, Patrick M., and Nicholas J. Matzke. 2013. "Primary Endosymbiosis Events Date to the Later Proterozoic with Cross-Calibrated Phylogenetic Dating of Duplicated ATPase Proteins." *Proceedings of the National Academy of Sciences of the United States of America* 110 (30): 12355–60.

Sowa, Yoshiyuki, and Richard M. Berry. 2008. "Bacterial Flagellar Motor." *Quarterly Reviews of Biophysics* 41 (02): 103–32. https://doi.org/10.1017/S0033583508004691.

Sowa, Yoshiyuki, Alexander D. Rowe, Mark C. Leake, Toshiharu Yakushi, Michio Homma, Akihiko Ishijima, and Richard M. Berry. 2005. "Direct Observation of Steps in Rotation of the Bacterial Flagellar Motor." *Nature* 437 (7060): 916–19.

Sugiyama, S., E. J. Cragoe, and Y. Imae. 1988. "Amiloride, a Specific Inhibitor for the Na+-Driven Flagellar Motors of Alkalophilic Bacillus." *The Journal of Biological Chemistry* 263 (17): 8215–19.

Terashima, Hiroyuki, Akihiro Kawamoto, Yusuke V. Morimoto, Katsumi Imada, and Tohru Minamino. 2017. "Structural Differences in the Bacterial Flagellar Motor among Bacterial Species." *Biophysics and Physicobiology* 14 (0): 191–98.

Uyeda, Josef C., Rosana Zenil-Ferguson, and Matthew W. Pennell. 2018. "Rethinking Phylogenetic Comparative Methods." *Systematic Biology* 67 (6): 1091–1109. //d

Wilson, David, and Anthony D. Keefe. 2000. "Random Mutagenesis by PCR." In *Current Protocols in Molecular Biology*, edited by Frederick M. Ausubel, Roger Brent, Robert E. Kingston, David D. Moore, J. G. Seidman, John A. Smith, and Kevin Struhl. John Wiley & Sons, 2003.

Yakushi, Toshiharu, Junghoon Yang, Hajime Fukuoka, Michio Homma, and David F. Blair. 2006. "Roles of Charged Residues of Rotor and Stator in Flagellar Rotation: Comparative Study Using H+-Driven and Na+-Driven Motors in Escherichia Coli." *Journal of Bacteriology* 188 (4): 1466–72.

Yonekura, Koji, Saori Maki-Yonekura, and Michio Homma. 2011. "Structure of the Flagellar Motor Protein Complex PomAB: Implications for the Torque-Generating Conformation ▿ ." *Journal of Bacteriology* 193 (15): 3863–70.

Yorimitsu, Tomohiro, and Michio Homma. 2001. "Na+-Driven Flagellar Motor of Vibrio." *Biochimica et Biophysica Acta (BBA) - Bioenergetics* 1505 (1): 82–93.

Zhu, Shiwei, Masato Takao, Na Li, Mayuko Sakuma, Yuuki Nishino, Michio Homma, Seiji Kojima, and Katsumi Imada. 2014. "Conformational Change in the Periplamic Region of the Flagellar Stator Coupled with the Assembly around the Rotor." *Proceedings of the National Academy of Sciences of the United States of America* 111 (37): 13523–28.

Author Contributions

TI collected and analysed data. RI collected and analysed data. JC collected data. NJM analysed data and wrote the manuscript. YS conceived and supervised the project, collected and analysed data, and wrote the manuscript. MABB conceived and supervised the project, collected and analysed data, and wrote the manuscript.

Funding Sources

NJM was supported by ARC DECRA fellowship DE150101773 and Marsden grants 16-UOA-277 and 18-UOA-034. YS was supported by JSPS KAKENHI (18H02475 and 15K07034), MEXT KAKENHI (15H01332), Ito Science Foundation, and Casio Science Promotion Foundation. MABB was supported by a UNSW Scientia Research Fellowship, a CSIRO Synthetic Biology Future Science Platform 2018 Project Grant and ARC Discovery Project DP190100497.